

PAPER • OPEN ACCESS

## Ultrasonic Tomography of Brick Columns Based on FEM Calculations

To cite this article: Monika Zielinska and Magdalena Rucka 2019 *IOP Conf. Ser.: Mater. Sci. Eng.* **471** 052039

View the [article online](#) for updates and enhancements.



**IOP | ebooks™**

Bringing you innovative digital publishing with leading voices to create your essential collection of books in STEM research.

Start exploring the [collection](#) - download the first chapter of every title for free.

# Ultrasonic Tomography of Brick Columns Based on FEM Calculations

Monika Zielinska <sup>1</sup>, Magdalena Rucka <sup>2</sup>

<sup>1</sup> Faculty of Architecture and Faculty of Civil and Environmental Engineering, Technical University of Gdansk, ul. Narutowicza 11/12, 80-233 Gdansk, Poland

<sup>2</sup> Faculty of Civil and Environmental Engineering, Technical University of Gdansk, ul. Narutowicza 11/12, 80-233 Gdansk, Poland

monika.zielinska@pg.edu.pl

**Abstract.** Ultrasonic tomography is one of the most developed method of non-destructive testing. Despite being used mainly in medicine, it is becoming more and more popular as a method for monitoring of structural elements. It allows to examine the internal structure and technical condition of the tested element. This paper investigates the influence of cross-sectional geometry on an obtained tomographic image. Wave propagation signals were obtained using finite element method (FEM). The analysis was conducted on six models of solid brick columns with a square section. The first one constituting a reference model was made in the form of a full column. The other models contained internal inclusions affecting propagating waves such as: a hole or a steel plate, circular bar and square pipe adhesively bonded with mortar. The obtained results of the analysis presented in the study allowed to assess the ultrasonic tomography usability for masonry structures.

## 1. Introduction

Brick structures are one of the most frequently used elements in engineering objects. They are mainly found in the form of walls, columns, ceilings or vaults. As slender elements, masonry columns are responsible for a proper transfer of large loads in relation to their small cross-section. They are often used by the architects as elements enabling the achievement of large, open spaces (figure 1). However, their application may have some consequences. Even the slightest weakening of this structural element can lead to a catastrophic failure of the whole object. An example of weakening of columns can be found in Saint Mary's Church in Gdansk [1]. During reconstruction of vaults some columns began to crack what became a reason for taking strong repairing and strengthening actions. Damages of the brick structures are also often caused by the material age, excessive loads and environmental factors, such as moisture or temperature. Any external damage is easy to detect and repair, while hidden structural defects are the biggest problem.

The paper is devoted to the subject of the ultrasonic wave propagation in brick columns. The study aims to assess the effectiveness of ultrasonic tomography in imaging of masonry structures. The influence of material discontinuities in the form of holes of various sizes and positions was investigated. The effect of steel elements embedded inside columns on ultrasonic waves was also studied. For this purpose, a circular bar, a plate and a square tube were introduced in the models. The conducted analysis aimed at taking preliminary steps to assess the technical condition of masonry columns. It indicated the possibility to detect discontinuities and elements that may be found inside the



column. The paper evaluated the opportunity to use ultrasonic examination as a basis for brick structures modernization or reinforcement works planning.



**Figure 1.** Examples of columns in churches in Gdansk, Poland:

a) St. John's Church, b) St. Brygida's Church, c) St. Mary's Church, d) St. Catherine's Church

## 2. Ultrasonic tomography

Ultrasonic waves are one of the most developed and comprehensive non-destructive testing methods. They are very popular in medicine for inspection of soft tissues. In civil engineering structures, guided ultrasonic waves are widely used to detect of damages in thin-walled structures like plates or shells (e.g. [2-5]). In methods based on wave propagation, time signals are usually registered at few selected points distributed on an examined structure. Therefore, an appropriate imaging making possible detection of potential damage is of great importance.

The ultrasonic tomography allows to visualize the internal structure of a given element based on the wave propagation signals acquired on its opposite sides. The tomography conducted on masonry structures is one of the most difficult tasks set for this method. The reason is the combination of two materials (bricks and mortar) which significantly complicates imaging in comparison to this carried out on single material, e.g. on concrete structures [6]. The ultrasonic tomography is mainly used for slab elements based on the Lamb waveforms [7-8]. This method is less often used to examine wooden elements [9], because wood anisotropy hinders the measurements performance on such elements. An example of the ultrasonic tomography application in stone blocks columns is described in [10].

In the tomography technique, the image is obtained after dividing the examined structure into small fragments, so-called pixels. A given pixel can be defined as an element with a specific wave transition

velocity if at least one wave beam passes through it. The collected data of the wave transition time for a given element form a basis for solving the equation:

$$t_i = \sum_j \frac{x_{ij}}{v_j} \quad (1)$$

where  $t_i$  is the transition velocity of the  $i$ -wavepath between a transmitter and a receiver,  $x_{ij}$  is the wave transition way and  $v_j$  denotes the waveform velocity through  $j$  pixel.

The measured transition time of the  $i$ -wave path is therefore the combined transition time values of waves passing through individual pixels on the wave's path. The aim of the ultrasonic tomography is to find a matrix representing the wave transition velocity passing through  $1,2,\dots,j$  pixels. In resulting tomography image various colours are used to represent elements with different wave propagation velocity.

In this study, tomographic imaging based on the iterative ART method (algebraic reconstruction techniques) is utilized. This method involves the determination of the iterative velocity matrix in each pixel, until the minimum measurement error is obtained. The use of iterative methods grows with the increase in the ability of computer technology and performance. The efficiency of these methods is constantly at the stage of development.

### 3. Description of columns

The analysis was carried out on six brick columns with dimensions of  $38 \times 38 \text{ cm}^2$  made of solid brick (figure 2). Each of them was characterized by a different geometry of the cross-section. The first model (# a), as a reference specimen, was made in the form of a full column. Bricks with dimensions of  $25 \times 12 \text{ cm}^2$  were connected with a 1 cm thick mortar. The next two models contained a hole arranged eccentrically (# b) and centrally (#c). The centrally located hole with dimensions of  $12 \times 12 \text{ cm}^2$  replaced the half brick in the full column. The eccentric hole had dimensions  $5.3 \times 5.3 \text{ cm}^2$ . The rest of the columns contained steel elements: a rod with a diameter of 32mm (#d), a plate of dimensions  $25 \times 2 \text{ cm}^2$  (# e), a square pipe with external dimensions of  $12 \times 12 \text{ cm}^2$  and a wall thickness of 15 mm (#f).

In order to perform numerical analysis on masonry elements it is crucial to properly select the material parameters of bricks and the mortar combining them. Literature suggests different propositions of parameters adopted for modelling such elements. Table 1 presents the values of Young's modulus for mortars and brick proposed by different authors.

**Table 1.** Young modulus for brick and mortar

| Authors                    | $E_{\text{brick}}[\text{MPa}]$ | $E_{\text{mortar}}[\text{MPa}]$ |
|----------------------------|--------------------------------|---------------------------------|
| Antoine [11]               | 11000                          | 2200                            |
| Lee et al. [12]            | 22000                          | 7400                            |
| Lourenço [13]              | 20000                          | 2000                            |
| Zucchini and Lourenço [14] | 20000                          | $1 < E_{\text{mor}}/E_b < 1000$ |
| Cluni and Gusella [15]     | 12500                          | 1200                            |
| Gabor et al. [16]          | 13000                          | 4000                            |
| Alberto et al. [17]        | 14500                          | 19500                           |
| Giamundo et al. [18]       | 1600                           | 111.41                          |
| Stefanou et al. [19]       | 6740                           | 1700                            |
| Rekik et al. [20]          | 10000                          | 0.489                           |

In this paper the Young's modulus and the Poisson's coefficient for mortar and brick were adopted according to paper [11]. The average value of Young's modulus necessary to model the gypsum mortar into which a bar was glued, was established from the tests described in [21]. The parameters for the materials used in the numerical study are summarized in table 2.

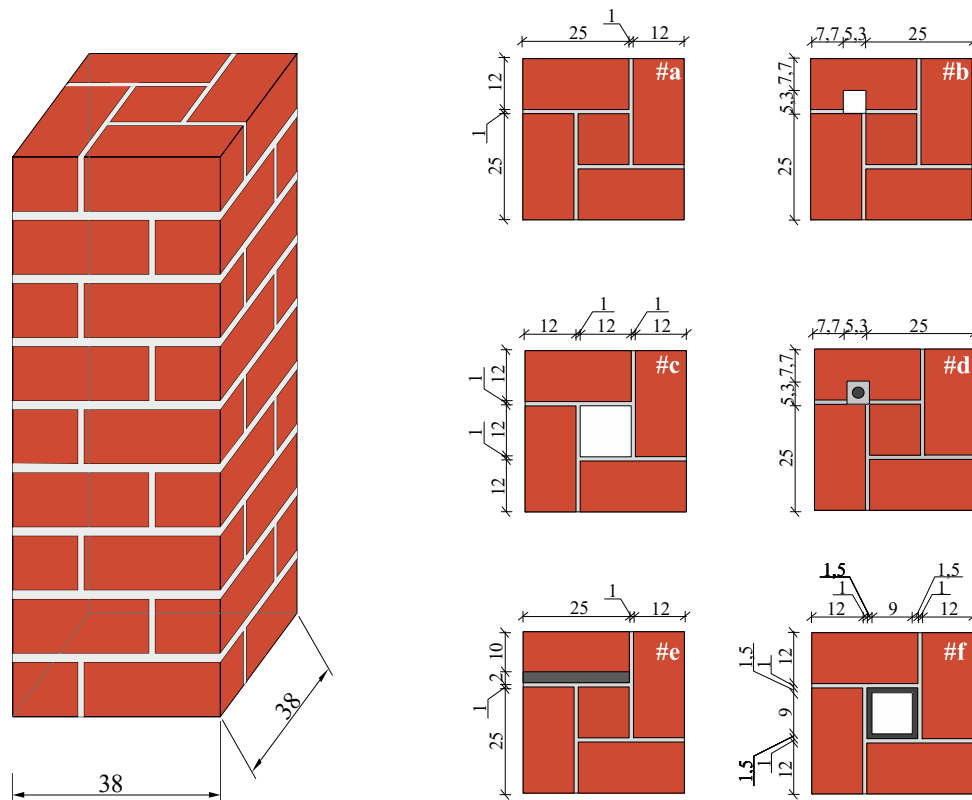


**Figure 2.** Geometry of brick columns: full column (#a), columns with hole (#b and #c), column with rod (#d), with plate (# e) and with square pipe (#f)

**Table 2.** Parameters of the materials

|               | Young modulus $E$ [MPa] | Poisson ratio $\nu$ | Density $\rho$ [kg/m <sup>3</sup> ] |
|---------------|-------------------------|---------------------|-------------------------------------|
| Brick         | 11 000                  | 0.20                | 1900                                |
| Mortar        | 2 200                   | 0.25                | 2100                                |
| Gypsum mortar | 585                     | 0.25                | 2100                                |
| Steel         | 200 000                 | 0.3                 | 7850                                |

The choice of material parameters has a direct impact on the test results, since the wave velocity depends on the value of the Poisson's coefficient, the Young's modulus and the density. The velocity of longitudinal waves in an isotropic medium can be determined in accordance with the following formula:

$$v = \sqrt{\frac{E(1-\nu)}{\rho(1+\nu)(1-2\nu)}} \quad (2)$$

For the brick used for the numerical tests the longitudinal velocity equals 2536 m/s, whereas for the mortar it is 1121 m/s.

#### 4. FEM calculations

The research assessing the influence of the sectional geometry on the ultrasonic tomography image was performed by means of a numerical analysis based on the finite element method (FEM). Analysis of wave propagation were carried out with commercial software Abaqus Explicit. All elements were modelled using four-node plane strain elements. Maximum size of the elements was assumed as 1 x 1

mm<sup>2</sup>. The surface contact between the brick and the mortar was adopted as a tie constraint. The boundary conditions were assumed as free of all edges. The excitation signal was implemented as the time-varying concentrated load in the form of 100 kHz wave packet modulated by the Hanning window, consisting of five sinusoid cycles (figure 3a). It was applied successively to points T (figure 3b) perpendicular to the edge of the column. Signals were also read in the direction perpendicular to the column surface. Time step of numerical integration was assumed as 100 ns due to the stability condition of the central difference method.

In the numerical study transmitters were located in 14 points (T<sub>1</sub>-T<sub>14</sub>), seven on each of the two adjacent walls of the column (figure 3b). The signal reading points were located on the opposite walls of the input signal. The readings were made in points S<sub>1</sub>-S<sub>7</sub> for each of the signals transmitted in T<sub>1</sub>-T<sub>7</sub> points. Analogously, for signals excited in points T<sub>8</sub>-T<sub>14</sub>, the time histories were registered in points S<sub>8</sub>-S<sub>14</sub>. The conducted numerical analysis allowed to collect 98 wave propagation signals. The transition time from the transmitter to the receivers of each wave was summarized on their basis.

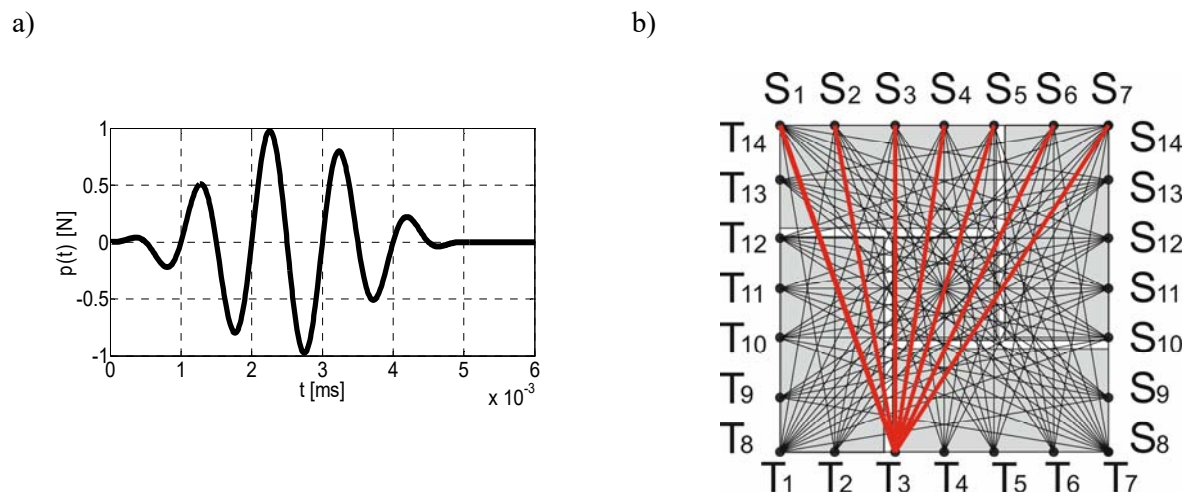


**Figure 3.** a) Excitation signal, b) position of transmitters (T<sub>1</sub> to T<sub>14</sub>) and sensors (S<sub>1</sub> to S<sub>14</sub>) during registration of ultrasonic waves

## 5. Results

Figure 4 illustrates the maps obtained from the ultrasonic tomography. The maps were calculated using the iterative ART method. Straight rays of registered waveforms without taking into account their curvature resulting from the encountered obstacles were adopted for the analysis. Each of the maps approximately localize the internal inclusions in the column. The holes can be identified as elements with a lower wave transition velocity than the column itself, whereas steel inserts caused the increase of the wave transition velocity. The mortar joint revealed the lowest velocities in the full column. The tomographic images made for columns with holes (#b and #c) clearly indicate their locations. Additionally, joints arrangement can be observed. The map for the model with eccentric hole (#b) is similar to the map for the model with the steel bar (#d). It is caused by a decrease in the velocity at the area of gypsum mortar, which properties reduce the waveform velocity. The maps for models with plate and pipe (#e and #f) revealed a significant increase of the wave velocity in locations of steel inserts. The tomography images obtained for these models indicated much higher propagation velocities than in the other columns.

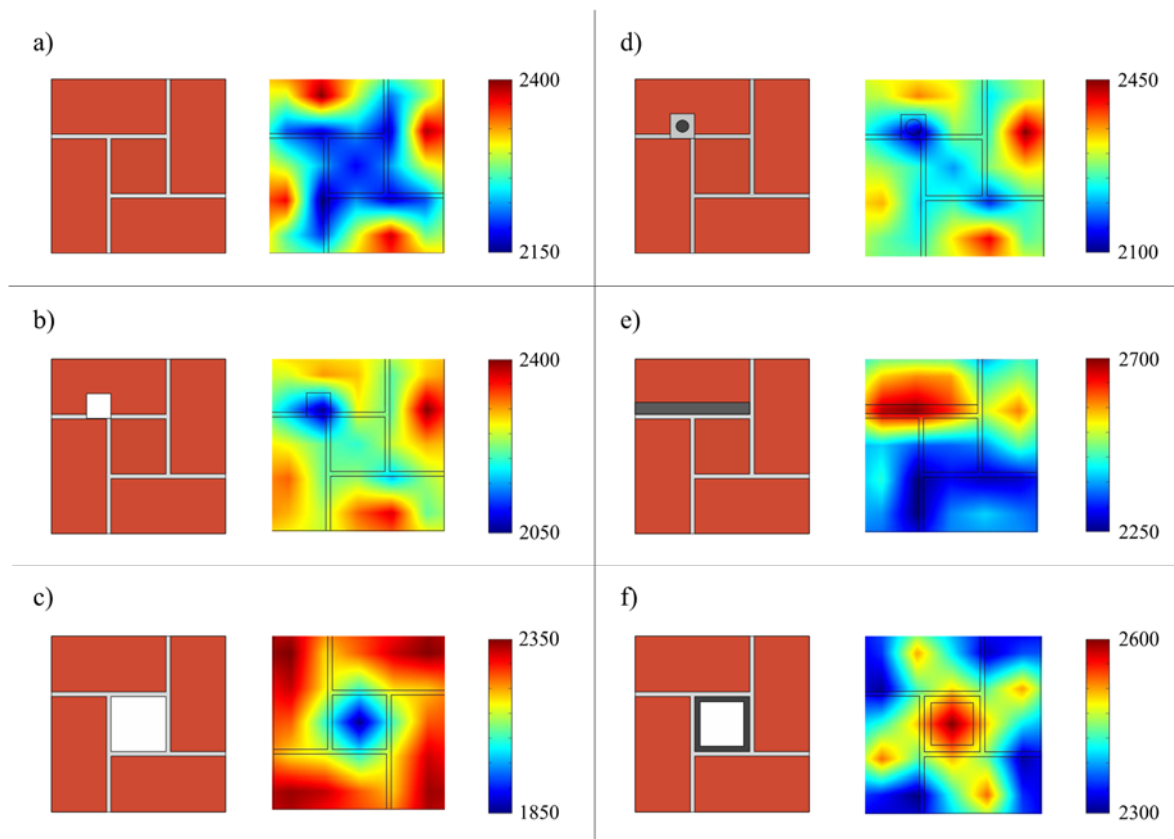


**Figure 4.** The ultrasonic tomography maps for columns with different sectional geometry

Table 3 lists the minimum, maximum, and average velocities of the wave transition for each of the investigated models. The lowest propagation velocity was recorded for the masonry model with a centrally located hole. A slightly higher minimum value was observed for the model with the eccentric hole. The velocity significantly increased for models with steel inserts. The highest velocity was recorded for the element with the steel plate.

**Table 3.** Wave transition velocities for the tested models #a-#f

| Model | $v_{\min}$ [m/s] | $v_{\max}$ [m/s] | $\Delta v$ [m/s] |
|-------|------------------|------------------|------------------|
| #a    | 2160.8           | 2439.3           | 2292.8           |
| #b    | 1986.5           | 2439.3           | 2272.0           |
| #c    | 1983.2           | 2423.4           | 2256.3           |
| #d    | 2039.3           | 2433.8           | 2273.0           |
| #e    | 2163.5           | 2994.2           | 2355.1           |
| #f    | 2169.9           | 2592.2           | 2353.4           |

## 6. Conclusions

The technical condition assessment of masonry structures using non-destructive methods is an extremely complicated task. It requires not only does appropriate devices, but also a huge knowledge necessary to correctly interpret the collected data. An accurate analysis of the obtained results can greatly facilitate the condition assessment of a given structure and the selection of a plan for reconstruction actions.

The numerical analysis presented in this study proved that the geometry of the examined sections had a significant influence on the obtained tomographic images. They confirmed that the use of the ultrasonic tomography tests can be applied to inspect the internal structure of not only structures made

with a single material, but also the elements composed of several materials. Additionally, it helped to recognize internal inclusions which is especially useful in the case of historic buildings with no available object design documentation. The research conducted on the example of masonry columns revealed the possibility of detecting both hole defects and steel inserts. The results obtained in this paper form the basis for further research in the field of understanding and modelling of masonry elements subjected to the ultrasonic testing.

## References

- [1] M. Rucka, J. Lachowicz, M. Zielińska M, “GPR investigation of the strengthening system of a historic masonry tower”, *Journal of Applied Geophysics*, vol. 131, pp. 94-102, 2016.
- [2] P.S.Tua, S.T.Ouek, Q. Wang, “Detection of cracks in plates using piezo-actuated Lamb waves”, *Smart Materials and Structures*, vol. 13, pp.643-660, 2004.
- [3] A. Žak, M. Krawczuk, W. Ostachowicz, “Propagation of in-plane waves in an isotropic panel with crack”, *Finite elements in Analysis and Design*, vol.42, pp. 929-941, 2006.
- [4] M. Rucka, B. Zima, R. Kędra, “Application of guided wave propagation in diagnostics of steel bridge components”, *Archives of Civil Engineering*, vol. LX, pp. 493-515,2014.
- [5] H. Peng, G. Meng, F. Li, “Modeling of wave propagation in plate structures using three-dimensional spectral element method for damage detection”, *Journal of Sound and Vibration*, vol. 320, pp. 942-954, 2009.
- [6] V. G. Haach, F. C. Ramirez, “Qualitative assessment of concrete by ultrasound tomography”, *Construction and Building Materials*, vol. 119, pp. 61–70, 2016.
- [7] S. Mahadev Prasad, Krishan Balasubramaniam, C V Krishnamurthy, “Structural health monitoring of composite structures using Lamb wave tomography”, *Smart Materials and Structures*, vol. 13, pp. 73-79, 2004.
- [8] X. Zhao, R. L. Royer, S. E. Owens, J. L. Rose, “Ultrasonic Lamb wave tomography in structural health monitoring”,*Smart Materials and Structures*, vol. 20, pp. 1-10, 2011.
- [9] C. Colla, “Verification of sonic tomography outcome through local testing of mechanical properties in historic timber beam”, *Journal of Heritage Conservation*, vol. 47, pp. 71-79, 2016.
- [10] V. Pérez-Gracia, J.O. Caselles, J. Clapés, G. Martinez, R. Osorio, “Non-destructive analysis in cultural heritage buildings: Evaluating the Mallorca cathedral supporting structures”, *NDT&EInternational*, vol. 59, pp.40–47, 2013.
- [11] A. Anthoine, “Derivation of the in-plane elastic characteristics of masonry through homogenization theory”, *International Journal of Solids and Structures*, vol. 32, no. 2, pp. 137–163, 1995.
- [12] J. S. Lee, G. N. Pande, J. Middleton, B. Kralj, “Numerical modelling of brick masonry panels subject to lateral loadings”, *Computers & Structures*, vol. 61, no. 4, pp. 735–745, 1996.
- [13] P. Lourenço, “Computational Strategies for Masonry Structures”, Delft University Press, Delft, The Netherlands, 1996.
- [14] A. Zucchini and P. B. Lourenço, “A micro-mechanical model for the homogenisation of masonry”, *International Journal of Solids and Structures*, vol. 39, no. 12, pp. 3233–3255, 2002.
- [15] F. Cluni and V. Gusella, “Homogenization of non-periodic masonry structures”, *International Journal of Solids and Structures*, vol. 41, no. 7, pp. 1911–1923, 2004.
- [16] A. Gabor, A. Bennani, E. Jacquelin, and F. Lebon, “Modelling approaches of the in-plane shear behaviour of unreinforced and FRP strengthened masonry panels”, *Composite Structures*, vol. 74, no. 3, pp. 277–288, 2006.
- [17] A.Alberto, P.Antonaci, S. Valente, “Damage analysis of brick-to-mortar interfaces”, *Procedia Engineering*, vol. 10 pp. 1151-1156, 2011.
- [18] V. Giamundo, V. Sarhosis, G.P. Lignola, Y. Sheng, G. Manfredi, “Evaluation of different computational modelling strategies for the analysis of low strength masonry structures”,



- Engineering Structures*, vol. 73, pp. 160-169, 2014.
- [19] I. Stefanou, K. Sab, and J.-V. Heck, “Three dimensional homogenization of masonry structures with building blocks of finite strength: a closed form strength domain”, *International Journal of Solids and Structures*, vol. 54, pp. 258–270, 2015.
- [20] A. Rekik, S. Allaoui, A. Gasser, E. Blond, K. Andreev, S. Sinnema, “Experiments and nonlinear homogenization sustaining mean-field theories for refractory mortarless masonry: the classical secant procedure and its improved variants”, *European Journal of Mechanics, A/Solids*, vol. 49, pp. 67–81, 2015.
- [21] J. Gontarz, J. Podgórski, „Examination of mechanical properties of porous gypsum” (in Polish), *Budownictwo i Architektura*, vol. 14(4) pp. 43-54, 2015.